Supporting Information

Synthesis and electronic properties of comb-like polyamides bearing different content of tetraaniline pendants

Mingying Yin[a], Ying Yan[a], Fangfei Li[b], Xincai Liu[a], Ce Wang[a], Danming Chao[a,*]

[a]*Alan G. MacDiarmid Institute, College of Chemistry, Jilin University, Changchun, 130012,P.R.China.*

[b]*State Key Lab of Superhard Materials, Jilin University, Changchun 130012, P.R.China.*

E-mail: chaodanming@jlu.edu.cn (D Chao), Tel.: +86-431-85168292; Fax: +86-431-85168292.

Experimental section

Materials.

N-Phenyl-*p*-phenylenediamine and 2,6-difluorobenzoyl chloride were purchased from Aldrich. 3,3',4,4'-Oxydiphthalic dianhydride (ODPA) was purchased from Shanghai Research Institute of Synthetic Resins. Ferric chloride, ammonium persulfate, potassium carbonate, sodium chloride, hydrochloric acid (37%) and ammonia water (25%) were obtained from Tianjin Chemical Factory. *N,N*′-Dimethylacetamide (DMAc), *N*,*N*′-dimethylformamide (DMF), dimethyl sulfoxide (DMSO), *N*-methyl-2-pyrrolidone (NMP), tetrahydrofuran (THF), toluene, acetone and ethanol were purchased from commercial sources and used as received without further purification. Optically transparent Indium-Tin Oxide (ITO) glass substrates were obtained from Reintech electronic technologies Co. Ltd (Beijing) and used as working electrode substrate in the electrochemical experiments. The composition of stainless steel (SS, T301), used in the anticorrosion tests, is as following (wt%): C 0.15%, Si 1.0%,Mn 2.0%, Cr16.0~18.0%, Ni6.0~8.0%,S 0.03%, P 0.045%and Fe bal.

General Methods.

Mass spectra were performed on an AXIMA-CFR laser desorption ionization flying time spectrometer (COMPACT). The ^{1}H NMR spectra of the obtained monomers and PXs in deuterated dimethyl sulfoxide were run on a Bruker-500 spectrometer at room temperature. Fourier-transform infrared spectra (FTIR) measurements were recorded on a BRUKER VECTOR 22 Spectrometer in the range of 4000-400 cm^{-1}. The composition of PXs were calculated from the results of elemental analysis. The weight percentages of carbon, hydrogen, nitrogen in the samples were measured by a Vario EL cube elemental analysis instrument. The molecular weight information of PXs was measured on Shimadzu Gel permeation chromatography (GPC) unit equipped with a Shimadzu GPC-802D gel column and SPD-M10AVP detector. *N,N'*-Dimethylformamide was used as the eluent at a flow rate of 1 mL/min. Thermogravimetric analysis (TGA) was carried out on a Perkin-Elmer PYRIS 1 TGA in the air atmosphere. Electrical resistivity of PXs was investigated on KEITHLEY 2400 via four-probe method. Dielectric properties of PXs were investigated in the range of 0.1 kHz-1 MHz on a Quad Tech Model 1920 LCR mete at room temperature. Cyclic voltammetry (CV) was investigated on a CHI 660A Electrochemical Workstation (CH Instruments, USA) with a conventional three-electrode cell, using an Ag/AgCl electrode as the reference electrode, a platinum wire electrode as the counter electrode, and the PXs/ITO as the working electrode. UV-vis spectra were performed on UV-2501 PC Spectrometer (SHIMADZU) in dilute PXs DMAc solution. The morphology of the obtained PXs film on ITO substrate was

characterized by a field-emission electron microscopy (SEM, FEI Nova Nano SEM).

Synthesis of tetraaniline

The synthetic route of tetraaniline had been reported in the literature [S1]. Its chracterization data was as follow:

FTIR (KBr, cm^{-1}): 3390 (s, υ_{N-H}), 3020 (m, υ_{C-H}), 1600 and 1527 (s, $\upsilon_{C=C}$ of benzenoid rings), 1305 (s, υ_{C-N}), 815 (m, δ_{C-H}), 746 (m, δ_{C-H}), 692 (m, δ_{C-H}). ^{1}H NMR (d_6-DMSO): δ=7.78 (s, 1H, due to –NH-), δ=7.68 (s, 1H, due to –NH-), δ=7.43 (s, 1H, due to–NH-), δ=7.12 (t, 2H, due to Ar-H), δ=6.87 (m, 12H, due to Ar-H), δ=6.65 (t, 1H, due to Ar-H), δ=6.51(d, 2H, due to Ar-H), δ=4.62 (s, 2H, due to $–NH_2$).

Synthesis of electroactive diamine monomer (EDA)

The synthetic route of EDA had been reported in the literature [S2]. Its chracterization data was as follow

MALDI-TOF-MS: m/z calculated for $C_{43}H_{36}N_6O_3$ = 684.8. Found 685.0. FTIR (KBr, cm^{-1}): 3380 (s,υ_{N-H}), 3037 (m, υ_{C-H}), 1657 (vs$\upsilon_{C=O}$), 1602 (s, $\upsilon_{C=C}$ of benzenoid rings), 1506 (vs $\upsilon_{C=C}$ of benzenoid rings), 1294 (s, υ_{C-N}), 1233 (m, υ_{C-O-C}), 829 (m, δ_{C-H}), 750 (m, δ_{C-H}), 696 (m, δ_{C-H}). ^{1}H NMR (d_6-DMSO): δ= 10.24 (s, 1H, due to –CONH-), δ= 7.74 (s, 1H, due to –NH-), δ= 7.69 (s, 1H, due to –NH-), δ= 7.60 (s, 1H, due to –NH-), δ= 7.54 (d, 2H, due to Ar-H), δ= 7.14 (t, 3H, due to Ar-H),δ= 6.93 (d, 12H, due to Ar-H), δ= 6.81 (d, 4H, due to Ar-H), δ= 6.67 (t, 1H, due to Ar-H), δ= 6.59 (d, 4H, due to Ar-H),δ= 6.29 (d, 2H, due to Ar-H), δ= 4.99 (s, 4H, due to -NH).

Synthesis of P1

A mixture of ODPA (6.2000g, 20 mmol), EDA (13.684g, 20 mmol) and 100 mL DMAc was added into 250 mL three-necked round-bottom flask under nitrogen atmosphere. The reaction proceeded with magnetic stirring at room temperature for 24 h. Then the resulting P1 DMAc solution was placed in the freezer at 5^{o}C and would be ready for synthesis of P2 and P3 material via post-functionalization method. Moreover, P1 was precipitated in the water, washed with deionized water and alcohol 2 times each, and then dried at 40 ^{o}C in the vacuum for 12 h. Characterization of P1: ^{1}H NMR (d_6-DMSO) (Fig.S1): δ =13.57-12.96 ppm (due to -COOH), δ =10.66-10.23 ppm (due to -CO-NH-), δ =7.46-7.73 ppm (due to -NH-), δ =7.51-6.46 ppm (due to Ar-H). FTIR (KBr, cm^{-1}): 3436 (υ_{N-H}), 1643 ($\upsilon_{C=O}$), 1569 and 1508 ($\upsilon_{C=C}$ of benzenoid rings), 1311 (υ_{C-N}), 1232 (υ_{C-O-C}), 819 (δ_{C-H}), 750 (δ_{C-H}), 676 (δ_{C-H}). Elemental analysis: Carbon (68.39%), Hydrogen (5.06%), Nitrogen (8.24), Ratio of Carbon and Nitrogen (calculated: 10.16; measured: 9.68). GPC data: Mw: 66280, PDI: 1.91.

Synthesis of P2

28.52 g P1 (5 mmol) DMAc solution was added into 50 mL three-necked round-bottom flask and cooled to 0-5 ^{o}C in the ice bath. Then 1 mL DMAP (0.1222g, 1 mmol) DMAc solution was added dropwise into the above solution. Ten minutes later, a mixture of tetraaniline (1.831g, 5 mmol), DCC (2.268g, 11mmol) and 4 mL DMAc was added dropwise into P1 DMAP solution within 30 minutes. Finally, the reaction proceeded with magnetic stirring under nitrogen at room temperature for 24 h. After that, P2 was precipitated in the water, and washed with deionized water,

dichloromethane and ethanol 2 times each. It was dried at 40 ^{o}C under the vacuum for 12 h. Characterization of P2: ^{1}H NMR (d_6-DMSO) (Fig.S1): δ =13.45-12.91 ppm (due to -COOH), δ =10.79-10.14 ppm (due to -CO-NH-), δ =7.89-7.66 ppm (due to -NH-), δ =7.53-6.42 ppm (due to Ar-H). FTIR (KBr, cm^{-1}): 3434 (υ_{N-H}), 1647 ($\upsilon_{C=O}$), 1585 and 1502 ($\upsilon_{C=C}$ of benzenoid rings), 1309 (υ_{C-N}), 1234 (υ_{C-O-C}), 837 (δ_{C-H}), 748 (δ_{C-H}), 673 (δ_{C-H}). Elemental analysis: Carbon (71.02%), Hydrogen (4.66%), Nitrogen (9.87), Ratio of Carbon and Nitrogen (calculated: 8.50; measured: 8.39). GPC data: Mw: 90320, PDI: 2.15.

P3 could be synthesized readily with increased amount of the chemicals using the same post-functionalization procedure. Characterization of P3: ^{1}H NMR (d_6-DMSO) (Fig.S1): δ =10.81-10.18 ppm (due to -CO-NH-), δ =7.46-7.73 ppm (due to -NH-), δ =7.50-6.41 ppm (due to Ar-H). FTIR (KBr, cm^{-1}): 3444 (υ_{N-H}), 1643 ($\upsilon_{C=O}$), 1565 and 1509 ($\upsilon_{C=C}$ of benzenoid rings), 1311 (υ_{C-N}), 1232 (υ_{C-O-C}), 819 (δ_{C-H}), 750 (δ_{C-H}), 676 (δ_{C-H}). Elemental analysis: Carbon (70.30%), Hydrogen (4.72%), Nitrogen (10.52), Ratio of Carbon and Nitrogen (calculated: 7.79; measured: 7.79). GPC data: Mw: 110880, PDI: 2.37.

Fabrication of the PXs/ITO electrodes and PXs/SS corrosive electrodes.

ITO substrates were prepared with 5.5×1 cm dimension and washed ultrasonically with acetone, distilled water and absolute ethyl alcohol for 3 min each, followed by drying in the air. PXs DMAc solution was filtered through 0.2-μm syringe filter, and then spin-coated onto the ITO substrate for electroactivity and electrochromism

measurements. The spin-coating process started at 500 rpm for 10 s and then 1000 rpm for 30 s.

The SS substrates with 2.0×1.0×0.1 cm dimension were polished with emery papers and washed ultrasonically with acetone, distilled water and ethanol for 3 min each, followed by drying in an oven. The filtered PXs DMAc solution was coated on the SS substrate for the anticorrosive tests. The coatings with increased thickness was obtained by casting onto SS substrates and then dried in the air.

Solubility of PXs

The solubility was determine with 5wt % solid content at 25 ^{o}C. The PXs are soluble in a variety of common polar solvents including tetrahydrofuran, dimethyl formamide, dimethyl acetamide (DMAc), dimethyl sulfoxide, and N-methyl-2-pyrrolidinone due to the bulky pendants in the molecular architecture. The visual difference was obvious and was presented in the Supporting Information (Fig.S2).

Thermal properties of PXs

As shown in Fig. S3, the P1 TGA curve shows a very clear two-step decomposition path. The first step loss occurs in the temperature range 130–270 °C with a mass loss of 12%, due to the dehydration of imidization cyclization. The subsequent weight loss occurs in the temperature range 300–740 °C with a mass loss of 85%, which could be associated to the decomposition of main chain. In the P2 curve, the first step loss occurs in the temperature range 170–300 °C with a mass loss of 4%, which is also due to the dehydration of imidization cyclization. The subsequent weight loss occurs in the temperature range 300–740 °C with a mass loss of 96%, which could be

associated to the decomposition of main chain. In the P3 curve, the first step loss occurs in the temperature range 150-250 ^{o}C with a mass loss of 2%, which is due to expulsion of loosely bounded water and solvent from the polymer chain. The loss occurs in the temperature range 300–760 °C with a mass loss of 98%, which could be associated to the decomposition of main chain.

Spectral properties

These spectroscopic properties exhibit interesting variation with the changing of oxidation states. Hence, the optical properties of P1 during the oxidation process were investigated by UV-vis spectroscopy. At the LEB state, only one strong absorption at 328 nm was observed in the UV-vis spectra (Fig. S5a), associated with a π–π* transition of the conjugated ring system [S3,S4]. When the oxidization took place in P1 DMAc solution by addition of trace amount of ammonium persulfate, the absorption of the π–π* transition continually decreased in intensity and underwent a blue shift. Meanwhile, a new absorption peaks appeared at 580 nm in the spectra, which is ascribed to the π-polaron transition [S3,S4]. With the oxidization of P1, the absorption at 580 nm continually increased in intensity. When the tetraaniline segments was oxidized to the EB state with tatraaniline containing one quinoid ring (Scheme S1), the intensity of π-polaron transiting absorption reached a maximum. Then the absorption of π-polaron transition began to undergo a red shift from 580 nm to 660 nm (Fig. S5b), but the absorption of the π–π* transition kept the blue shift to 288 nm with decreasing intensity. After reaching the PNB state with two quinoid

rings in the tetraaniline segment (Scheme S1), all the absorption peaks remained unchanged. The chemical oxidation process is consistent with that of oligoaniline and polyaniline, due to the similar oligoaniline units as the electroactive item. P2 and P3 exhibited the similar chemical oxidation process except for the absorption ratio of 580 nm to 328 nm. The ratio of P1, P2 and P3 is 32.36%, 38.82%, 40.50%, respectively, which is due to the increasing of tetraaniline content in polymers' structure.

Supporting Figures.

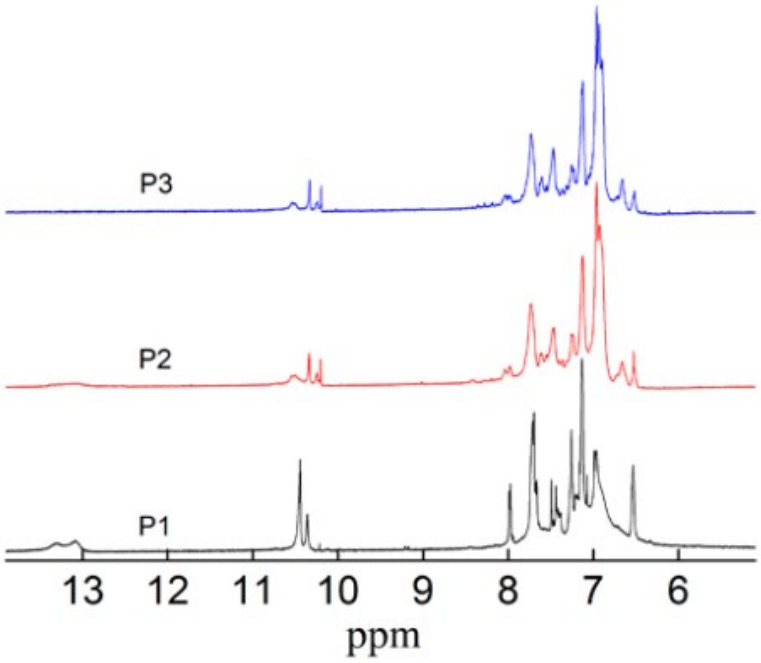

Fig. S1: ^{1}H NMR spectra of PXs.

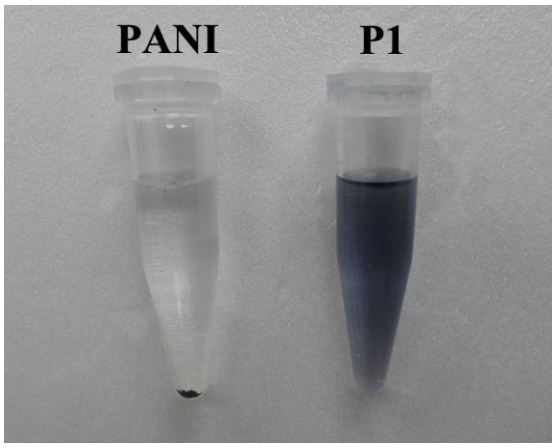

Fig. S2. Digital image of polyaniline and P1s in DMAc with 5wt % solid content at 25 ^{o}C.

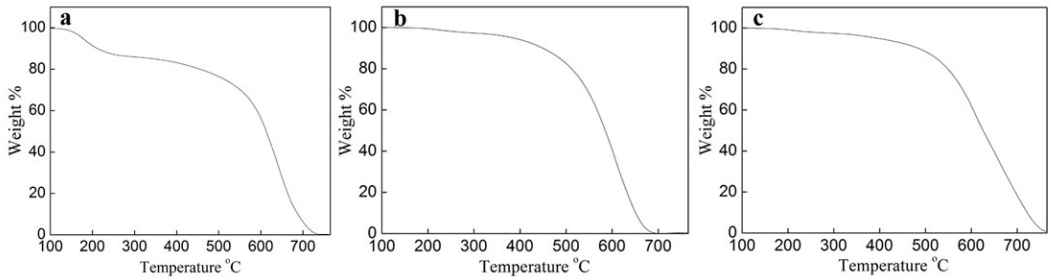

Fig. S3. TGA curves of P1 (a), P2 (b), and P3 (c) in air atmosphere.

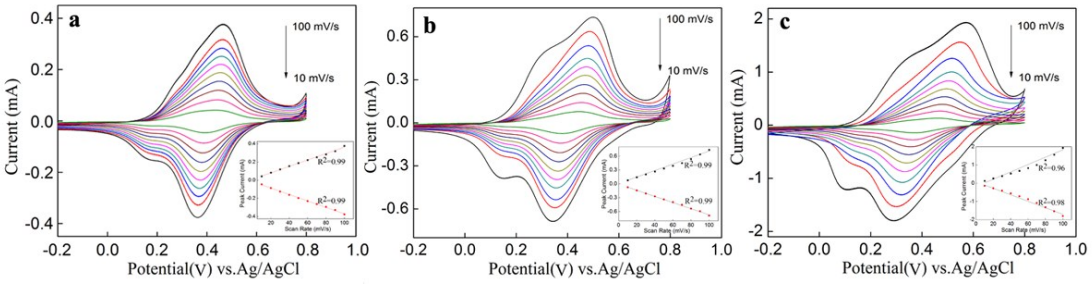

Fig. S4. CV of P1/ITO (a), P2/ITO (b), P3/ITO (c) electrodes in 0.5 M H_2SO_4 at different potential scan rates: 10-100 mV/s. Insets in each figure show the relationships between the oxidation and reduction current vs. potential scan rate.

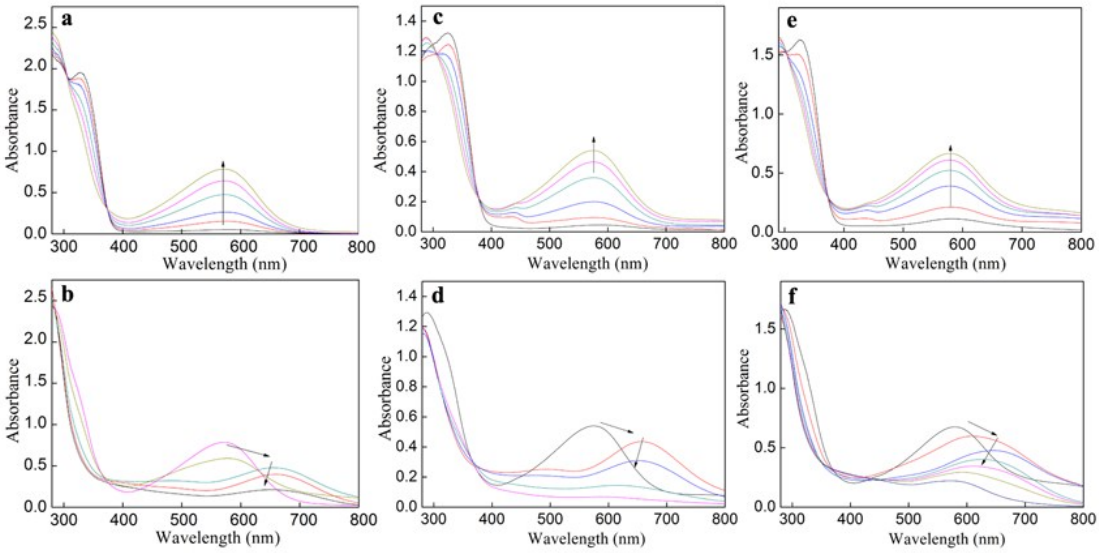

Fig. S5. UV-vis spectra monitoring the chemical oxidation of P1 (a and b), P2 (c and d), P3 (e and f) from LEB to EB and EB to PNB.

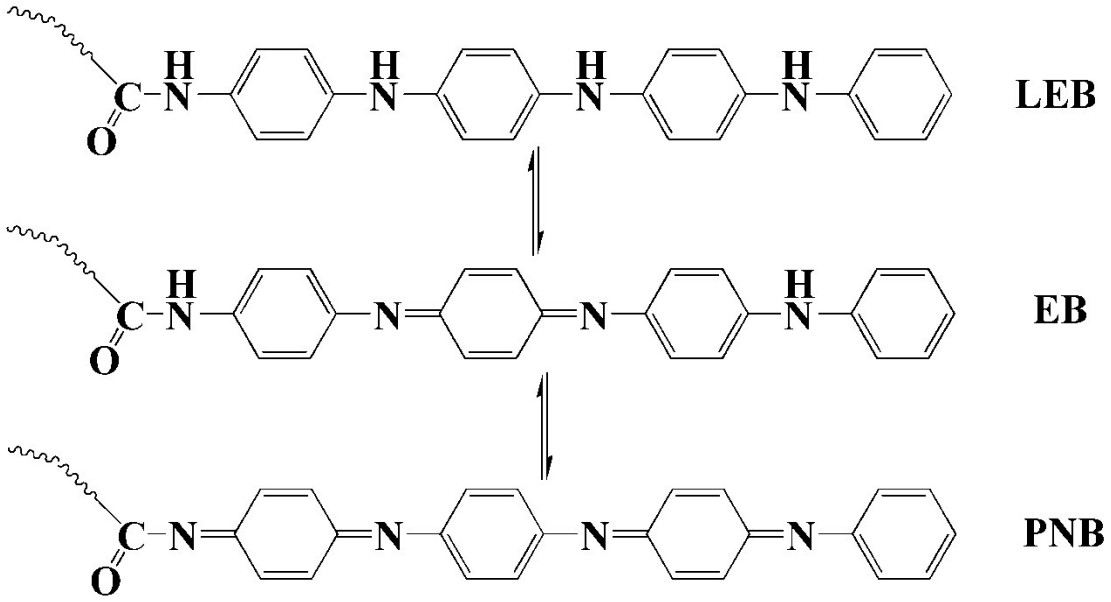

Scheme S1. The molecular structures of PXs at various oxidation states.

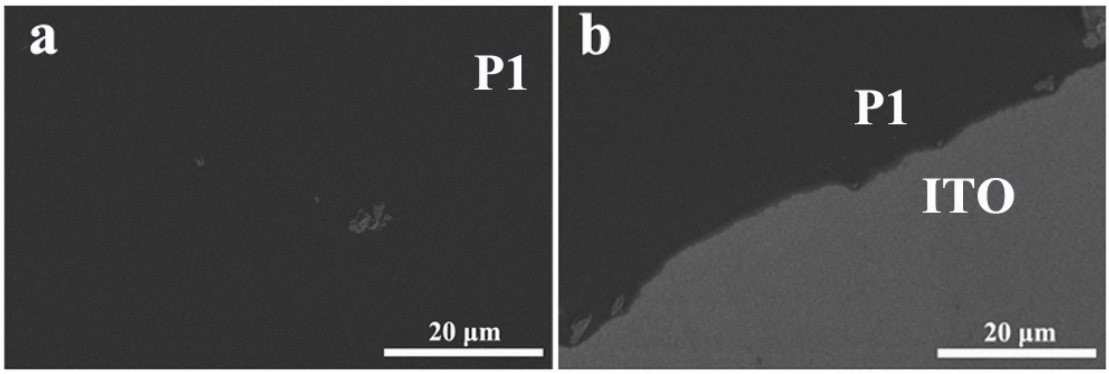

Fig. S6. SEM image of the spin-formed P1 layer (a) and the boundary region of P1 on the ITO substrate.

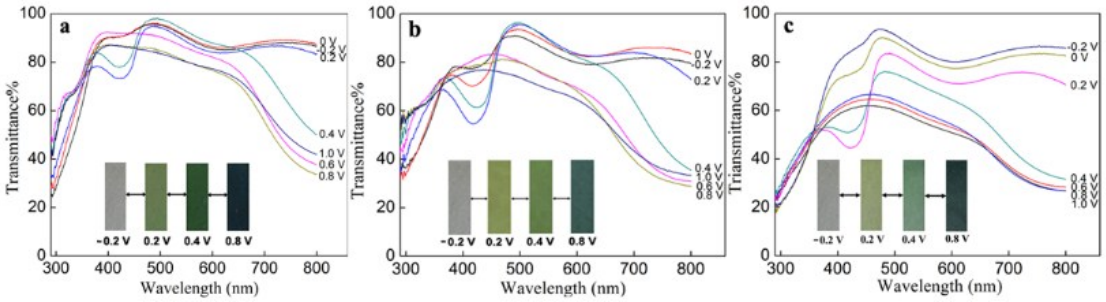

Fig. S7. The spectral changes of the P1/ITO (a), P2/ITO (b), P3/ITO (c) electrodes in 0.5 mol/L H_2SO_4 at different potentials.

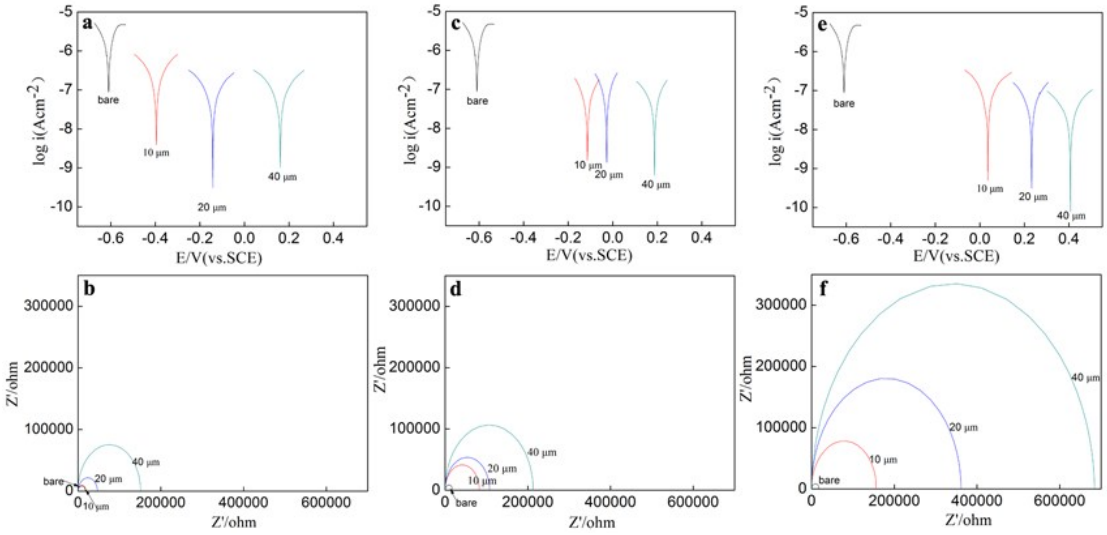

Fig. S8. Tafel plots and EIS for P1/SS (a and b), P2/SS (c and d), P3/SS (e and f) corrosive electrodes with various thicknesses (10 μm, 20 μm, and 40 μm).

Sample	E_{Corr}(V)	I_{Corr}(μA/cm^2)	R_p(kΩ cm^2)	R_{Corr}(mm/year)	P_{ef}(%)
0	-0.610	6.085	0.06118	4.868×10^{-2}	——
P1-10μm	-0.396	0.3606	2.984	2.775×10^{-3}	97.95
P1-20μm	-0.142	0.2429	4.408	1.870×10^{-3}	98.61
P1-40μm	0.161	0.1326	8.073	1.021×10^{-3}	99.24
P2-10μm	-0.114	0.1689	4.931	1.300×10^{-3}	98.75
P2-20μm	-0.001	0.1679	6.860	1.292×10^{-3}	99.11
P2-40μm	0. 188	0.1196	8.927	9.206×10^{-4}	99.31
P3-10μm	0.036	0.1686	5.611	1.297×10^{-3}	98.91
P3-20μm	0.233	0.1024	10.35	7.882×10^{-4}	99.41
P3-40μm	0.407	0.05033	21.07	3.874×10^{-4}	99.71

Table S1. Electrochemical corrosion parameters of the PXs/SS samples with various thicknesses (10 μm, 20 μm, and 40 μm) in 3.5 wt% NaCl solution.

Sample	10μm	20μm	40μm
P1	18752 Ω	47329 Ω	150975 Ω
P2	82721 Ω	107439 Ω	212662 Ω
P3	155657 Ω	361505 Ω	684325 Ω

Table S2. R_f of PXs/SS samples with various thicknesses (10 μm, 20μm, and 40 μm) in 3.5 wt% NaCl solution. The R_f of SS is 10742 Ω.

References:

[S1] D. Chao, X. Jia, H. Liu, L. He, L. Cui, C. Wang, E. B. Berda, J. Polym. Sci., Part A: Polym. Chem., 2011, 49, 1605–1614.

[S2] X. Jia, D. Chao, H. Liu, L. He, T. Zheng, X. Bian, C. Wang, Polym. Chem. 2011, 2, 1300–1306.

[S3] S. D. Ohmura, T. Moriuchi, T. Hirao, J. Org. Chem., 2010, 75, 7909-7912.

[S4] L. W. Shacklette, J. F. Wolf, S. Gould, R. H. Baughman, J. Chem. Phys., 1988, 88, 3955-3961.